

Effect of Inorganic Pigments on Polymer Interdiffusion in a Low- T_g Latex Film

Mitsuru Kobayashi,[†] Yahya Rharbi, and Mitchell A. Winnik*

Department of Chemistry, University of Toronto, 80 St. George Street, Toronto, Ontario, M5S 3H6 Canada

Received April 4, 2000; Revised Manuscript Received November 29, 2000

ABSTRACT: There is a continuing need to lower costs of coated paper production while at the same time maintaining or improving paper quality. To reach this goal, one would like to have the knowledge necessary to design the structure of the coating in a way that optimizes the use of latex as a pigment binder. For this purpose, one needs a deeper understanding of the role of the latex binder in the coating. We approach this problem by trying to understand how a large amount of pigment in the coating formulation affects the coalescence of latex particles and the subsequent polymer diffusion that enhances the mechanical properties. We carried out fluorescence resonance energy transfer (FRET) measurements on latex films that allowed us to follow the extent of interparticle polymer diffusion as a function of time after the latex/pigment dispersion dried. The initial energy-transfer quantum efficiency data indicate that neither precipitated calcium carbonate (CaCO_3) nor silica (SiO_2) promotes coalescence of the latex particles. CaCO_3 has little effect on the rate of polymer interdiffusion up to 80 wt %, whereas even a small amount of 25-nm silica particles has a significant influence.

Introduction

Latex polymer is widely used as a pigment binder for various types of coated papers.¹ It is of significant importance to understand the factors that affect the structure of the coating, especially the spatial arrangement of the pigment particles and binder. These factors are important for the control of product quality and the design of new products.² Understanding latex particle deformation and the evolution of film properties is also important because these are the steps that promote adhesion to the inorganic pigment and adhesion to the cellulose fibers. The amount of binder in a paper coating is small, because of the relatively high cost compared to the cost of conventional pigments such as clay and calcium carbonate. Therefore, it is essential to optimize the characteristics of the latex, both to maintain or improve the quality of the paper and to lower the paper cost. It is well-known that, during the drying process, latex particles deform above the glass transition temperature (T_g) of the polymer to form a void-free solid composed of polyhedral cells. Over time, this cellular structure is lost as the polymer diffuses across the intercellular boundaries and creates a continuous polymer matrix.³ There have been a number of studies on wetting and adhesion of polymer latex particles to inorganic pigments in paper coatings.^{4–6} These include the scanning electron microscope studies by Scriven et al.⁵ and the recent neutron scattering study by Joanicot et al.⁶ Despite this effort, how the latex particles deform in the presence of large amounts of inorganic pigments during film formation is still not well understood.

Our research group has developed a quantitative technique based on fluorescent spectroscopy for studying polymer interdiffusion in latex films. In this technique, one mixes two essentially identical types of latex particles in dispersion prior to film formation. Both types

of latex particles are covalently labeled with about 1 mol % of a fluorescent dye, one with a dye that can act as a donor (D) in a fluorescence resonance energy transfer (FRET) experiment and the other with a corresponding acceptor dye (A).⁷ In a FRET experiment, the donor dye is excited selectively with light at a wavelength where it has a strong absorption. This excited dye can fluoresce, or, if there is a nearby acceptor dye, the energy can be transferred to the acceptor dye via a resonant coupling of the transition dipoles. The energy-transfer process occurs as described in eq 1. When a dispersion containing donor- and acceptor-labeled particles dries to form a film, some of the boundaries separate donor- and acceptor-labeled polymer. As these polymers diffuse across the boundaries, they bring donor and acceptor dyes into proximity, allowing the extent of energy transfer to increase.



Over the past 15 years, we have used this technique to examine a variety of factors that affect the rate of polymer diffusion in latex films. Most of these experiments were carried out on pigment-free dispersions, with the intent of understanding how the properties of the binder phase itself evolve.⁸ Recently, we began to examine the influence of pigments on the polymer diffusion rate in latex films. For example, Feng et al.⁹ found that hard polymer particles such as poly(methyl methacrylate) (PMMA) and Ropaque (Rohm & Haas) significantly retard the rate of polymer interdiffusion. Here, we extend these studies to mineral fillers as pigments in latex films and consider a broader range of pigment content. In most paints, the amount of pigment is sufficiently small that polymer binder is the continuous phase. In paper coatings, the amount of pigment exceeds the critical pigment volume concentration, and the coating contains a significant fraction of air voids. In this paper, we describe the application of FRET measurements to the study of the polymer interdiffusion process in latex films that contain large amounts of

* To whom correspondence should be addressed. E-mail: mwinnik@chem.utoronto.ca.

[†] Permanent address: Pulp and Paper Research Laboratory, Oji Paper Co., Ltd., 4-3-1, Jokoji, Amagasaki, Hyogo, 660-8577, Japan.

Table 1. Recipes for Preparing 110-nm P(MMA–EHA) Latex

	first stage (batch process)	second stage (under monomer-starved conditions)	
		Phe-labeled	MeAn-labeled
MMA (g)	1.75	17.5	17.5
EHA (g)	1.75	17.5	17.5
MeAn-MMA (g)			0.78 ^a
Phe-MMA (g)		0.75 ^a	
water (g)	58.8	27.0	27.0
KPS (g)	0.06	0.06	0.06
SDS (g)	0.10	0.61	0.61
1-dodecanethiol (g)		0.07	0.07
NaHCO ₃ (g)	0.06		
<i>T</i> _{React} ^b (°C)	80	80	85
<i>t</i> _{React} ^c (h)	2	20	20

^a 1 mol % relative to the total monomer fed in the second stage was added. ^b Reaction temperature. ^c Reaction time.

inorganic pigments, typical of those used in paper coatings. We show that calcium carbonate pigment and silica have very different effects on the rate of polymer diffusion in these films.

Experimental Section

Latex Samples. Methyl methacrylate (MMA) and (2-ethylhexyl) acrylate (EHA) were distilled under vacuum prior to use. Potassium persulfate (KPS), sodium bicarbonate (NaHCO₃), sodium dodecyl sulfate (SDS), and 1-dodecanethiol were used as supplied. Distilled water was further purified through a Millipore Milli-Q system. Poly(MMA–EHA) copolymer latex samples (monomer weight ratio of 1:1), labeled with 1 mol % of a fluorescent dye [either a donor, phenanthrene (Phe) or an acceptor, anthracene (An)], were prepared by semicontinuous emulsion copolymerization at 80 °C, using KPS as the initiator, SDS as the surfactant, and 1-dodecanethiol as the chain-transfer agent. The reaction conditions were similar to those described previously.¹⁰ We used (9-phenanthryl)methyl methacrylate (Phe) to introduce the donor dye. The synthesis of this monomer is described in ref 11. As an acceptor-labeled monomer, we used 9-methacryloxymethyl-10-methylanthracene (MeAn), recently developed by Liu et al. for emulsion polymerization of acrylate monomers.¹²

The recipe for preparing 110-nm latex particles is shown in Table 1. We used the same seed latex particles obtained in the first stage for preparing both the Phe- and MeAn-labeled latex particles. The particle size and size distributions were determined by dynamic light scattering employing a Brookhaven BI-90 particle sizer. Molecular weight and molecular weight distributions were measured by gel permeation chromatography (GPC), using two Ultrastaygel columns (500 × 10⁴ Å) with tetrahydrofuran (THF) as the eluent and a flow rate of 0.4 mL/min. These polymers were calibrated based on poly(methyl methacrylate) (PMMA) standards. Dual detectors (refractive index and fluorescence detectors) were used to detect the presence of the donor and acceptor dyes and to ensure that these fluorescent dyes are randomly distributed in the polymer backbone. The glass transition temperatures (*T*_g) of the polymers were determined by differential scanning calorimetry (DSC) (Perkin-Elmer DSC-7), with a heating rate of 10 °C/min and with the samples under N₂. The characteristics of the polymers are shown in Table 2. These latex particles, referred to as P(MMA–EHA), have a diameter of 110 nm and a *T*_g of 7 °C. The solids content of the dispersion was measured gravimetrically and was found to be ca. 30 wt %.

Inorganic Pigments. Precipitated calcium carbonate (TP-221GS, Okutama Kogyo Co., Ltd), dispersed with sodium polyacrylate, was supplied as a suspension in water. This pigment has an ellipsoidal shape, termed scalenohedral calcite, with a length of 0.7–1.0 μm and a diameter of 0.25–0.3 μm. This pigment is commonly used for high-gloss coated paper. Colloidal silica (Klebosol 30R25, Clariant Corporation) was

Table 2. Characteristics of the Latex Particles and Inorganic Pigment Particles

	P(MMA–EHA) ^a	precipitated calcium carbonate	colloidal silica
diameter (nm)	110	250–300 ^b	25
<i>T</i> _g (°C)	7	—	—
10 ^{−4} <i>M</i> _w	24	—	—
10 ^{−4} <i>M</i> _n	5.2	—	—
<i>M</i> _w / <i>M</i> _n	4.6	—	—
pH	5.8	10.5	9.0

^a Both the Phe- and the MeAn-labeled latex particles have almost identical characteristics. ^b The lengths of the pigment particles are 700–1000 nm.

supplied as a suspension in water. The filler particles are amorphous spherical silica beads with a diameter of around 25 nm and a narrow size distribution.¹³ The particles show good dispersibility in water. Both pigments were used as supplied. Further pigment characteristics are shown in Table 2.

Film Formation and Measurements. Latex films were prepared from dispersion mixtures with a 1:1 number ratio of Phe- and MeAn-labeled P(MMA–EHA) latex particles and different amounts of inorganic pigment. The final dispersions, with total solids contents from ca. 30 to 60 wt %, were adjusted to pH 9 with diluted potassium hydroxide solution for the dispersions with SiO₂ and those without pigment and with diluted hydrochloric acid solution for the dispersions with CaCO₃. Film formation was carried out by the following procedure. For each film, we took three drops of each dispersion using a Pasteur pipet and spread them onto a quartz plate. Then, we leveled off those dispersions using a stainless steel blade. Then film was allowed to dry for 10 min in air at 23 °C and then stored in a cold room at 4 °C to minimize the amount of polymer interdiffusion in the film. A typical film thickness was 100 μm. Films formed from latex alone were crack-free and transparent. The films became more turbid as the amount of precipitated calcium carbonate increases. All films containing colloidal silica were transparent and crack-free up to 40 wt %, and small cracks were observed in the film containing 50 wt % of silica. All films were annealed at 50 ± 1 °C for polymer interdiffusion measurements. For each series of samples to be compared, the films were annealed simultaneously.

Fluorescence decay profiles were measured by the single-photon-timing technique.¹⁴ Samples were excited at 300 nm, and emission was detected at 350 nm. A band-pass filter (350 ± 5 nm) was used to minimize the scattered light and interference due to fluorescence from directly excited acceptors. For each measurement, it took about 10–15 min to collect 5000 counts in the maximum channel. Prior to each measurement, a film sample was placed in a quartz tube, and the tube was degassed with flowing nitrogen gas.

Because of the high pigment content, many of the films that we examine are turbid or even opaque. For these films, the extent of light penetration into the film is limited. Because of a relatively large extent of light scattering in opaque samples, the depth of light penetration might be as small as the wavelength of the excitation light (here 300 nm). Therefore, one needs to align the optics carefully to minimize the amount of scattered light reaching the detector. Because the scattered light has shorter wavelengths than the emitted light, proper use of filters can minimize its contribution to the measured decay. We excite the donor at 300 nm and detect the emission at 350 nm with a band-pass filter (350 ± 5 nm). Because scattered light has the same time profile as the excitation pulse, one can correct the measured decay profile for any residual contribution due to scattered light.¹⁵

Data and Data Analysis

The latex films that we examined were prepared from a 1:1 mixture of donor- and acceptor-labeled latex particles. We monitored the polymer diffusion process by measuring changes in the extent of energy transfer

between the donor and acceptor dyes attached to these latex polymers. When a donor dye D is excited, it can transfer its energy to any nearby acceptor dyes A. The important feature of this process is that the rate of energy transfer $w(r)$ depends sensitively on the distance r between the donor and acceptor molecules

$$w(r) = \frac{1}{\tau_D^0} \left(\frac{R_0}{r} \right)^6 \quad (2)$$

where τ_D^0 is the donor fluorescence lifetime in the absence of acceptors, and R_0 is the characteristic distance (the Förster distance) over which energy transfer takes place.³

For energy transfer for donors and acceptors randomly distributed in a three-dimensional Euclidean space, the donor decay function has a stretched exponential form⁷

$$I_D(t) = I_0 \exp\left(-\frac{t}{\tau_D}\right) \exp\left[-P\left(\frac{t}{\tau_D}\right)^{0.5}\right] \quad (3a)$$

where I_0 is the intensity at zero time and P is a parameter proportional to the local concentration of acceptors C_A

$$P = \kappa^2 \frac{4\pi^{3/2}}{3000} N_{Av} R_0^3 C_A \quad (3b)$$

where N_{Av} is Avogadro's number and κ^2 describes the averaged relative orientation of the donor and acceptor dipole moments.

In our experiments, we measure donor fluorescence decay profiles $I_D(t)$. To fit each decay curve, we use the following phenomenological equation:

$$I_D(t) = A_1 \exp\left[-\frac{t}{\tau_D^0} - p\left(\frac{t}{\tau_D^0}\right)^{0.5}\right] + A_2 \exp\left(-\frac{t}{\tau_D}\right) \quad (4)$$

Although this equation is similar in form to eq 3a, no meaning is ascribed to the individual fitting parameters. The parameters A_1 , A_2 , and p are obtained from the fit of each decay profile, and we use these fitting parameters to integrate $I_D(t)$ analytically from decay time $t = 0$ to $t = \infty$.

The efficiency of energy transfer, $\Phi_{ET}(t)$ is defined as shown in eq 5

$$\Phi_{ET}(t) = \frac{\text{number of ET events}}{\text{number of photons absorbed}} = 1 - \frac{\int_0^\infty I_D(t) dt}{\int_0^\infty I_D^0(t) dt} \quad (5)$$

where $\int_0^\infty I_D(t) dt$ is the area under the fluorescence donor decay profile obtained from the samples containing both D and A¹⁶ and $\int_0^\infty I_D^0(t) dt = \tau_D^0$. Equation 5 can be rewritten as

$$\Phi_{ET}(t) = 1 - \frac{\text{area}(t)}{\tau_D^0} \quad (6)$$

Although the extent of energy transfer can, in principle, be determined by measuring the intensities of donor and acceptor fluorescence, this experiment suffers from several artifacts, particularly the absorption by A

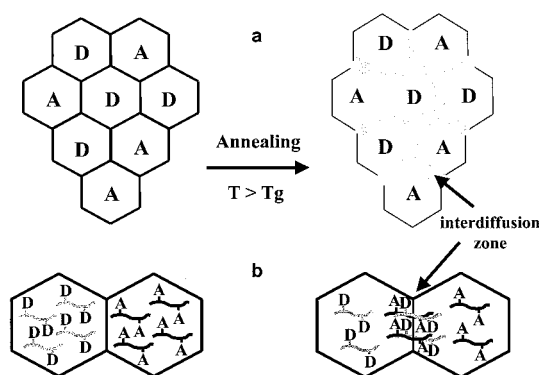


Figure 1. Schematic representation of polymer interdiffusion for a latex film. (a) When a latex film is annealed well above its glass transition temperature (T_g), a zone of interdiffusion develops, which contains mixtures of D- and A-labeled polymer molecules. (b) The D- and A-labeled polymer molecules interdiffuse across the cell boundary. Energy transfer can occur between the D and A chromophores that are close together.

of light emitted by the excited D. In our experiments, we avoid this problem by carrying out fluorescence decay experiments. We measure the influence of the acceptor dye on the decay rate of the donor dye following pulsed excitation. In the absence of acceptor, the phenanthrene chromophore that we employ as the donor dye undergoes an exponential decay with a lifetime τ_D^0 . In our analysis of the donor fluorescence decay data, we assume that all deviations from a strictly exponential donor decay profile are due to FRET. For the films that we examine here, $\tau_D^0 = 45$ ns.

Another useful parameter is the extent of mixing, $f_m(t)$, expressed in terms of the growth in energy-transfer efficiency, normalized by the maximum change associated with complete mixing.¹⁶

$$f_m(t) = \frac{\Phi_{ET}(t) - \Phi_{ET}(0)}{\Phi_{ET}(\infty) - \Phi_{ET}(0)} = \frac{\text{area}(0) - \text{area}(t)}{\text{area}(0) - \text{area}(\infty)} \quad (7)$$

where $[\Phi_{ET}(t) - \Phi_{ET}(0)]$ represents the change in the efficiency of energy transfer between the initially prepared film and a film annealed for time t .

Results

In Figure 1, we present a drawing of a planar section of an idealized latex film prepared from a mixture of D- and A-labeled latex particles in the absence of pigment. This type of ordered structure is obtained if the particles are uniform in size and self-organized into a face-centered-cubic array at a high solids content as the dispersion dries.¹⁷ When the latex film is annealed or allowed to age, polymer diffusion across the intercellular boundaries brings the donor- and acceptor-labeled polymers into proximity. A schematic representation of polymer interdiffusion across the intercellular boundary in a latex film is shown in part b of Figure 1. When two adjacent cells are labeled with D and A chromophores, polymer interdiffusion will bring the D and A dyes closer together. This process leads to a measurable increase in energy transfer.

In this report, we examine the influence of inorganic pigments on the interdiffusion rate. We use two types of inorganic pigments. One is precipitated calcium carbonate (CaCO_3) with a much larger diameter than the latex particles. The other pigment is colloidal silica (SiO_2) with a smaller diameter than the latex particles.

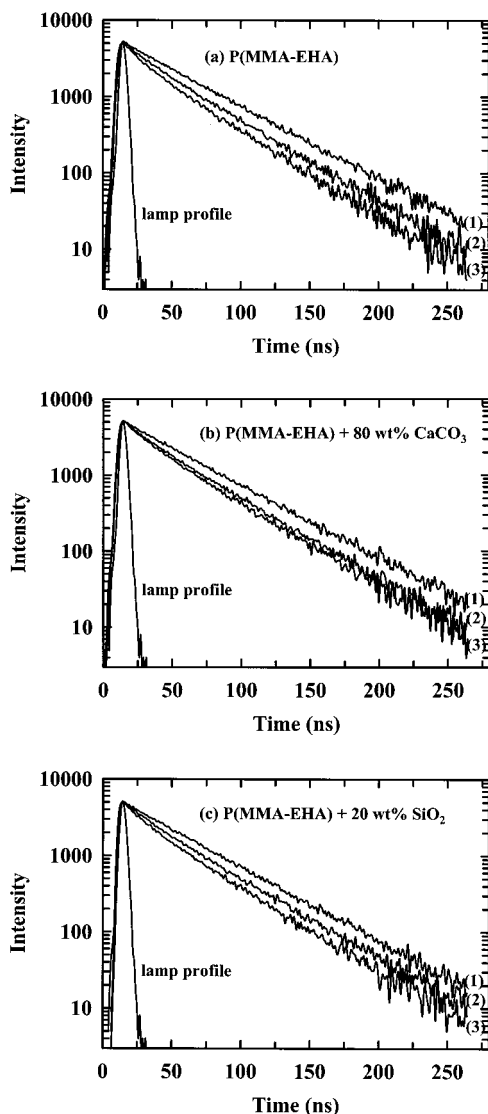


Figure 2. Donor fluorescence decay profiles (a) in a P(MMA-EHA) latex film without pigment, (b) in a latex film containing 80 wt % CaCO_3 , and (c) in a latex film containing 20 wt % SiO_2 . These films were annealed at $50 \pm 1^\circ\text{C}$ for (1) 0, (2) 60, and (3) 990 min. The individual decay profiles are fitted to eq 4 and then integrated analytically to obtain the area under each curve.

Those pigments might be expected to play different roles during the film-formation process. In the second stage of film formation, the latex particles are likely to be located between the CaCO_3 pigments, because the size of the CaCO_3 particles is much larger than that of the latex particles. On the other hand, SiO_2 might be located between the latex particles, because the size of SiO_2 particles is much smaller than that of the latex particles.

Typical donor fluorescence decay profiles in a latex film are shown in Figure 2. Figure 2a shows data obtained for a latex film containing no pigment. Figure 2b shows the corresponding decay traces obtained for a film containing 80 wt % CaCO_3 . Figure 2c shows the corresponding decay traces obtained for a film containing 20 wt % SiO_2 . When the latex film is annealed at temperatures well above T_g , polymer interdiffusion occurs. One can see the evolution of polymer interdiffusion in the films by looking at the extent of curvature of the decay profiles. As the film is annealed for longer times, the curvature becomes more pronounced, which indicates that polymer interdiffusion is promoted by

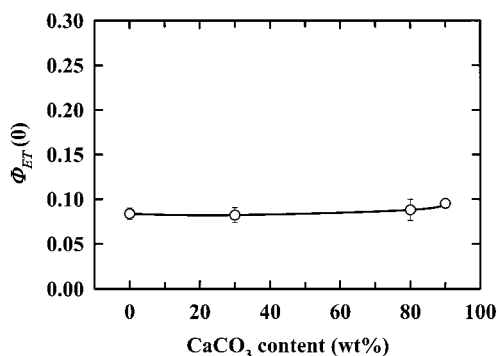


Figure 3. Effect of CaCO_3 fraction on the initial efficiency of energy transfer. We plot the initial energy-transfer quantum efficiency $\Phi_{\text{ET}}(0)$ vs weight percent of CaCO_3 in each latex film.

heat and annealing time. One can also see that, for similar annealing times, the extent of energy transfer for the films containing pigment is smaller than that for the films containing no pigment.

Efficiency of Energy Transfer $\Phi_{\text{ET}}(0)$ in Newly Formed Films. In this section, we examine the influence of pigment on the extent of energy transfer in newly formed films. If these films are prepared at low enough temperature, little or no polymer interdiffusion will take place. Energy transfer will occur only across the interface between cells formed by the D- and A-labeled latex particles. Under these circumstances $\Phi_{\text{ET}}(t=0)$ is a measure of the interfacial area between D- and A-labeled cells in the film.⁹ The newly formed films that we examined were allowed to dry at room temperature (23°C , i.e., above the minimum film-forming temperature), but as soon as the film appeared to be dry, it was transferred to a cold room at 4°C for storage until the decay profile of the cold film could be measured. Because the T_g of the matrix polymer is 7°C , we imagine that minimal polymer diffusion occurs when the films are prepared in this way. We use experimental values of $\text{area}(0)$ and $\Phi_{\text{ET}}(0)$ to examine the effect of pigment on the contact between D- and A-labeled latex particles in the newly formed films.

Effect of CaCO_3 . In Figure 3, we plot $\Phi_{\text{ET}}(0)$ vs CaCO_3 (wt %) for a series of freshly prepared films. The values of $\Phi_{\text{ET}}(0)$ obtained range from 0.082 to 0.095. In other experiments on nascent films prepared from similar-sized latex particles at temperatures close to the minimum film-forming temperature, $\Phi_{\text{ET}}(0)$ values on the order of 0.05 to 0.07 were obtained.¹⁸ These results suggest that little polymer diffusion has occurred in the samples that we have examined. Note also that meaningful data are obtained for films containing 80 and 90 wt % CaCO_3 . These films contain large amounts of air voids and, as a consequence, are opaque. By carefully aligning the optics for the measurement, the extent of light scattering reaching the detector is minimized. Some scattered light at the excitation wavelength is detected, but we correct its contribution to the fluorescence signal, as described in ref 15, by the software used for data analysis.

One can see in Figure 3 that the magnitude of $\Phi_{\text{ET}}(0)$ is essentially independent of the amount of CaCO_3 in the film. This result indicates that, even when large amounts of CaCO_3 are present, there is a common extent of interfacial contact in the film between cells formed from D- and A-labeled latex particles. One could imagine that wetting of the pigment by the latex

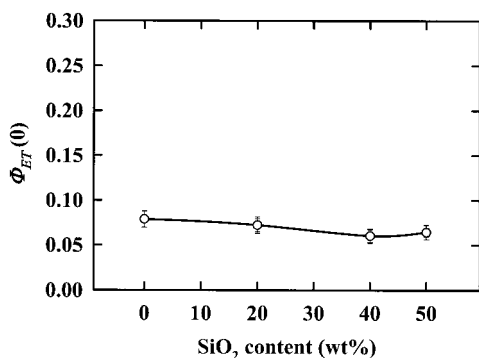


Figure 4. Effect of SiO₂ fraction on the initial efficiency of energy transfer. We plot $\Phi_{ET}(0)$ vs weight percent of SiO₂ in each latex film.

polymer might even promote the extent of mixing in the newly formed films. This does not occur. We conclude that CaCO₃ pigment does not promote coalescence of the latex particles.

Effect of SiO₂. In Figure 4, we plot values of $\Phi_{ET}(0)$ vs SiO₂ (wt %) for newly formed latex films. In the case of latex films containing CaCO₃, useful films could be prepared containing as much as 90 wt % pigment. Here, we were limited to films containing up to 50 wt % SiO₂. When we attempted to prepare films containing larger amounts of silica, those films were so brittle after they dried that they could not be handled. For the films whose results are shown in Figure 4, we obtained $\Phi_{ET}(0)$ values ranging from 0.060 to 0.079. The initial values of the energy-transfer quantum efficiency are slightly lower than those for CaCO₃ and appear to decrease slightly with increasing amounts of SiO₂. As we mentioned above, $\Phi_{ET}(0)$ is primarily a measure of the interfacial area between D- and A-labeled cells in the film. The data in Figure 4 indicate that the SiO₂ pigment with a diameter of 25 nm appears to have a small effect either on reducing the interfacial area between D- and A-labeled cells in the system or on suppressing the limited extent of polymer diffusion that occurs during film formation. Like CaCO₃, SiO₂ does not promote coalescence of the latex particles during film formation.

Maximum Efficiency of Energy Transfer $\Phi_{ET}(\infty)$ in Latex Films. To evaluate the extent of mixing, $f_m(t)$, defined by eq 7, we need to know the value of $\Phi_{ET}(\infty)$, which corresponds to full mixing of the donor- and acceptor-labeled polymer. In the energy-transfer experiments that we carry out, simulations have shown that Φ_{ET} reaches its maximum value when the polymers in the film diffuse a distance on the order of the original particle radius.¹⁹ There are two ways to obtain a sample, which will serve as a model for $\Phi_{ET}(\infty)$. First, one can take a film and anneal it for a sufficient time at a high temperature. Because the polymer rate is strongly accelerated by increasing temperature, Φ_{ET} will normally increase rapidly to its maximum value. Alternatively, one can dissolve a dry film sample in an organic solvent. In solution, one expects full mixing of the polymer molecules. A film cast from this solution is then a good model for the determination of $\Phi_{ET}(\infty)$. In pigment-free films, both approaches give similar results for the $\text{area}(\infty)$ values from which the corresponding $\Phi_{ET}(\infty)$ values are calculated.

For pigment-free P(MMA-EHA) latex films, we obtained $\text{area}(\infty)$ values from a solvent-cast film. This film was prepared from a dry latex film prepared from a 1:1

Table 3. Final Areas and Energy-Transfer Quantum Efficiencies of Latex Films in the Absence and Presence of Pigment

	CaCO ₃ (wt %)	t_{anneal}^a (min)	T_{anneal}^b (°C)	area^c (ns)	Φ_{ET}	
1	0	60	80	18.2	0.60	solvent cast
2	0	6750	50	22.6	0.50	
3	90	6750	50	30.5	0.33	
4	0	6750	60	19.7	0.57	
5	90	6750	60	29.3	0.36	6 + THF
6	90	30	100	26.1	0.42	
7	90	30	120	23.8	0.48	
8	90	30	140	24.5	0.46	
9	90	—	—	20.6	0.55	

^a Annealing time ^b Annealing temperature ^c Integrated area under the donor fluorescence decay profile

mixture of D- and A-labeled particles, which was subsequently dissolved in tetrahydrofuran (THF). The solution was cast onto a quartz plate and allowed to dry at room temperature for 12 h. For these films, we obtained $\text{area}(\infty) = 18.2$ ns and $\Phi_{ET}(\infty) = 0.60$, and these values did not change when the film was annealed at 80 °C for 1 h. In contrast, when a sample of the latex film itself was annealed at 50 °C for 112 h, we obtained an apparent $\text{area}(\infty)$ value of 22.6 ns and an apparent $\Phi_{ET}(\infty)$ value of 0.50. We infer from these results that, for prolonged annealing at 50 °C, full mixing is not achieved. As one can see in Table 3, a latex film heated at 60 °C for this length of time gave values closer to those found for the solvent-cast film, $\text{area}(\infty) = 19.7$ ns and $\Phi_{ET}(\infty) = 0.57$.

If the film is fully mixed, one should have a random distribution of donors and acceptors, and the decay profile should be described by eq 3a. Under these circumstances, the rate and efficiency of energy transfer will be determined only by R_0 , κ^2 , and the concentration of acceptors in the film. The fluorescence decay profile for the solvent-cast pigment-free latex film gave an excellent fit to eq 3a. Assuming immobile randomly oriented chromophores, we calculated the R_0 value from the magnitude of the fitting parameter P . We obtained $R_0 = 2.03$ nm if we assume that the concentration of acceptors in the film is 3.2×10^{-2} M, corresponding to a 1:1 number ratio of Phe- and MeAn-labeled latex particles.

In the following section, we examine the effect of pigment on the magnitude of Φ_{ET} after annealing for relatively long periods of time. Because these values are always smaller than the $\Phi_{ET}(\infty)$ values obtained for the pigment-free films, we refer to these apparent infinite-time values and denote them $\text{area}(\infty)$ and $\Phi_{ET}(\infty)$. This result was unexpected. As a consequence, we examined this effect in some detail, particularly for the films containing large amounts of CaCO₃.

As seen in Table 3, a film containing 90 wt % CaCO₃ annealed for 112 h at 50 °C had $\text{area}(\infty) = 30.5$ ns and $\Phi_{ET}(\infty) = 0.33$. When we repeated this experiment at 60 °C, $\Phi_{ET}(\infty)$ increased to 0.36, still well below the value expected for complete interdiffusion. Even annealing a film containing 90 wt % CaCO₃ for 30 min at 120 °C increased $\Phi_{ET}(\infty)$ to only 0.48. To force mixing, we added THF to a latex film containing 90 wt % CaCO₃. The polymer was kept in the presence of the solvent for several minutes, and then the solvent was allowed to evaporate. This film, after drying for 12 h at room temperature, had a significantly higher extent of energy transfer, $\Phi_{ET}(\infty) = 0.55$.

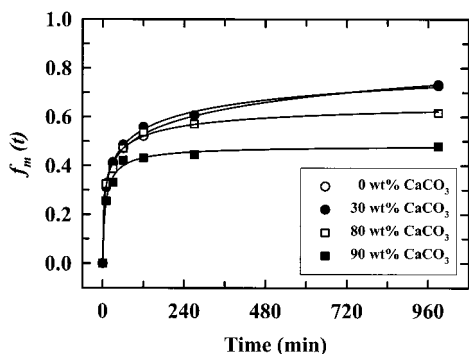


Figure 5. Comparison of P(MMA–EHA) diffusion rates for films containing different amounts of calcium carbonate, expressed as weight percentages: 0 (open circles), 30 (solid circles), 80 (open squares), and 90 (solid squares). We plot the extent of mixing, $f_m(t)$, vs the annealing time. The weight-average molecular weight (M_w) of the P(MMA–EHA) latex used was approximately 240 000. The films were annealed simultaneously at 50 ± 1 °C.

We also determined $\text{area}(\infty)$ values for films containing up to 50 wt % silica. For samples annealed for 112 h at 50 °C, these values ranged from 22.2 ns (no silica) to 28.7 ns (50 wt % of SiO_2), corresponding to $\Phi_{\text{ET}}(\infty)$ values from 0.51 to 0.37. As in the case of calcium carbonate, the presence of pigment appears to lower the energy-transfer quantum efficiency accessible by annealing the latex films at this temperature.

To examine the influence of pigment on the rate of polymer diffusion, we need to calculate values of $f_m(t)$. Because $f_m(t)$ is a measure of the extent of mixing in the system, we need to choose values for $\text{area}(\infty)$ and $\Phi_{\text{ET}}(\infty)$ that describe only the latex polymer in the system and are not influenced by any effect of the pigment on limiting the total extent of interdiffusion. For this reason, we use values obtained for the pigment-free polymer obtained by solvent casting, namely, $\text{area}(\infty) = 18.2$ ns and $\Phi_{\text{ET}}(\infty) = 0.60$.

Effect of Pigment on the Rate of Polymer Interdiffusion. In Figure 5, we plot the values of $f_m(t)$ as a function of annealing time at 50 °C for films containing different amounts of CaCO_3 . For these experiments, we assume that the annealing temperature of 50 °C does not affect the characteristics of CaCO_3 pigment. The $f_m(t)$ values were calculated via eq 7 from the areas under the fluorescent decay curves, using a common $\text{area}(\infty)$ value of 18.2 ns. The most important result in Figure 5 is that polymer interdiffusion is not substantially retarded by the presence of the CaCO_3 pigment. The diffusion rate is unchanged for amounts of pigment up to 30 wt %. Even at 80 wt %, the effect is relatively small, whereas 90 wt % CaCO_3 has a significant effect at reducing the diffusion rate of the latex polymer. Various experiments were repeated a number of times, and experiments were carried out at different temperatures. The trends shown in Figure 5 are consistent. For experiments to be meaningful, a set of samples must be annealed simultaneously. It is difficult to reproduce the exact profile of $f_m(t)$ vs t for experiments carried out at different times. The problem is one of reproducing the oven temperature. The polymer diffusion rate is so sensitive to temperature (with apparent activation energies ranging from 160²⁰ to 400 kJ/mol²¹) that even small temperature differences between experiments have a noticeable effect on the rates of polymer diffusion.

In Figure 6, we plot the values of $f_m(t)$ as a function of annealing time at 50 °C for films containing different

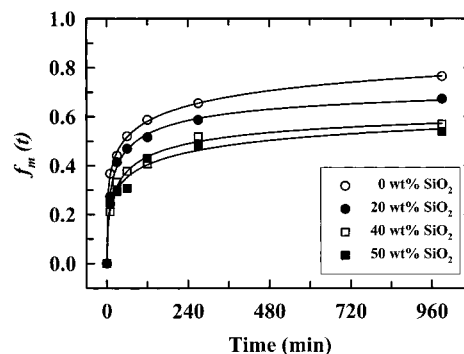


Figure 6. Comparison of P(MMA–EHA) diffusion rates for films containing different amounts of silica, expressed as weight percentages: 0 (open circles), 20 (solid circles), 40 (open squares), and 50 (solid squares). We plot the extent of mixing, $f_m(t)$, vs the annealing time. The films were annealed simultaneously at 50 ± 1 °C.

amounts of SiO_2 . Here, we see that the presence of smaller amounts of SiO_2 in the film have a pronounced effect on reducing the rate of polymer interdiffusion. There is greater retardation when one increases the amount of SiO_2 in the latex films.

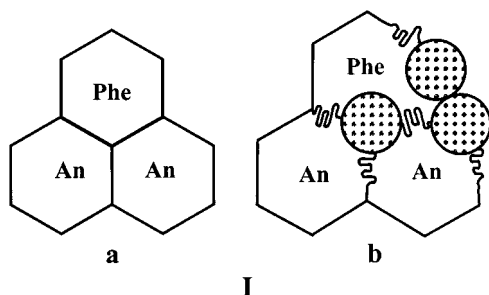
Discussion

The polymer that we examined as the binder for our model paper coatings is prepared from equal parts by weight of MMA and EHA using semicontinuous emulsion polymerization to maintain a uniform composition throughout the polymerization. The mole ratio of the MMA and EHA components is 65/35, and the polymer has a T_g of 7 °C. The seed particle used in the synthesis was prepared by batch emulsion polymerization in the absence of any chain-transfer agent, whereas a small amount of 1-dodecanethiol was added in the second stage to limit the molecular weight. A broad molecular weight distribution was found for these latex polymers by gel permeation chromatography (GPC). We know little about branching in the polymer that we produced. Given the reactivity of the polymerizing acrylate radical and the presence of the tertiary hydrogen on the EHA side chain, it is likely that the polymer that we examined contains substantial branching. Analysis of the latex polymer by GPC, using tandem fluorescence and refractive index detectors, establishes that the fluorescent dyes are covalently bound to the polymer and uniformly incorporated.

In pigment-free latex films, polymer diffusion is slow at room temperature but faster at 50 °C. Under these conditions, 43 °C above T_g , the initial stage of polymer diffusion [to $f_m(t) = 0.4$] is rapid, followed by a slower rate of increase. As mentioned above, the polymer molecular weight distribution is broad, and there is likely to be a distribution of branching as well. The smaller and more compact structures are likely to have faster intrinsic diffusion rates. In latex films containing a mixture of species with a distribution of diffusivities, the fastest diffusing species make the largest contribution to $f_m(t)$ at early times. One can, in principle, obtain a deeper insight into the nature of the diffusion process by assuming a model and calculating apparent diffusion coefficients. We will defer this type of analysis for a future report. The time necessary for full mixing is much longer than those shown in Figures 5 and 6. As seen in Table 3, even 6750 min (112 h) of annealing at $T_g + 43$ °C does not lead to full mixing. Here, $\Phi_{\text{ET}} = 0.50$,

whereas, for the fully mixed sample, prepared by solvent casting, $\Phi_{ET} = 0.60$. It might be that some of the polymers in the sample, as a consequence of long-chain branching, have a starlike structure. Such polymers have a very slow rate of diffusion in polymer melts.²²

Pigment Effects on $\Phi_{ET}(0)$. One of the most curious results obtained in our experiments concerns the magnitude of the quantum efficiency of energy transfer in newly formed films. We find that films formed in the presence of pigment exhibit almost no change in the value of $\Phi_{ET}(0)$ compared with the pigment-free films. These results are similar to those reported by Feng et al.,⁹ who found that $\Phi_{ET}(0)$ for linear poly(butyl methacrylate) (PBMA) latex films was unaffected by the presence of 35 vol % poly(methyl methacrylate) (PMMA) filler particles. Simulations suggest that the magnitude of $\Phi_{ET}(0)$ in pigment-free films depends on the amount of interfacial area between donor- and acceptor-labeled cells multiplied by the effective thickness of the interface between them.²³ $\Phi_{ET}(0)$ values on the order of 0.05–0.07 for latex films formed from 110-nm-diameter particles are consistent with intimate contact but little or no polymer diffusion between adjacent cells in the film, as shown as a in the drawing of species I.



In these filler-containing latex films, a significant fraction of the latex polymer surface is in contact with the filler particles. It is difficult to imagine how the latex particle can pack and yet maintain a constant interfacial area between donor- and acceptor-labeled cells. Recently, Odrobina et al.²⁴ have suggested that, when the latex particles deform to accommodate the filler particles, their deformation is accompanied by undulations in the interface between adjacent cells. In this way, the interfacial area between donor- and acceptor-labeled polymer is larger than that expected from simple polyhedral cells.

Pigment Effects on the Polymer Diffusion Rate.

We observe that, in the presence of pigment, the polymer diffusion rate is retarded. As one can see in Figures 5 and 6, silica is much more effective at decreasing the diffusion rate than CaCO_3 . It takes 20–40 wt % silica to have the same effect on the polymer diffusion rate as 80–90 wt % CaCO_3 . Our results are, in many ways, similar to those of Feng et al.,⁹ who studied the effect of PMMA particles (with a glass transition temperature $T_g \approx 100^\circ\text{C}$) on the rate of polymer diffusion in films prepared from PBMA. In their experiments, they examined films containing a constant fraction (35 vol %) of PMMA particles of different sizes. They found that the diffusion rate decreased in proportion to the increase in the surface area of the hard filler particles, i.e., with a decrease in the hard particle size at constant filler volume. We can attribute at least part of the larger effect of silica on the polymer interdiffusion rate in the films to its much larger surface area,

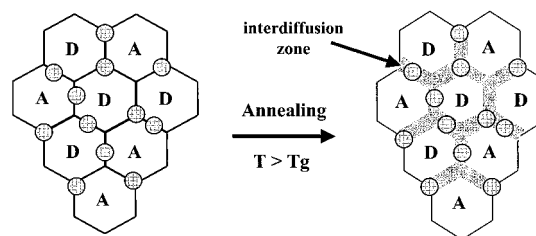


Figure 7. Schematic representation of the annealing process for a latex film containing 25-nm silica particles. The silica particles can act as obstacles to retard polymer diffusion. Strong interactions between the silica surface and the polymer can also reduce the mobility of polymer molecules near the pigment surface.

compared to films containing CaCO_3 where the surface-to-volume ratio is ca. 10 times smaller. In addition, the surfaces of the pigment are very different. The Si–OH groups at the surface of the silica are likely to be strong hydrogen bond donors toward the ester groups in the latex polymer.

There are two types of explanations for the effect of filler on a reduced polymer diffusion rate. In the first model, the hard pigment surface serves to make the adjacent polymer matrix more rigid. It is well-known that polymer chains adjacent to a strongly interacting rigid surface have decreased mobility.²⁵ Tsagaropoulos and Eisenberg²⁶ proposed a three-layer model in terms of polymer mobility. They studied changes in the glass transition temperature associated with the addition of small silica particles as fillers to various bulk polymers. As increasing amounts of filler were added, a new high glass transition temperature was found in addition to the T_g for the bulk polymer. As more filler was added, they found a decrease in the magnitude of the signal from which T_g was determined. In their model, the surface layer of polymer adjacent to the pigment is strongly immobilized, but in addition, nearby polymer also has its mobility restricted. It is this nearby polymer that contributes to the elevated T_g . From this perspective, one reason for the decreased rate of polymer diffusion found here is that the polymer molecules near the pigment surface have decreased mobility.

In the case of small silica particles as the pigment, another effect can become important. As shown in Figure 7, the silica particles are much smaller than the latex particles. When the film dries, one can imagine that the silica particles decorate the interface between adjacent cells. In this way, they can serve as obstacles to the diffusion of latex polymer. It is important to recognize that obstacles slow diffusion without affecting the intrinsic mobility of the diffusing species. Obstacles at an interface operate in a different way, and force molecules to diffuse along more tortuous pathways to reach the same extent of interdiffusion.²⁷ As a consequence, the time necessary for mixing is longer.

Figure 8 illustrates an important feature of the binder–pigment morphology when small amounts of binder are used with CaCO_3 as the pigment. At very high pigment levels, the binder is present as small droplets that glue individual pigment particles together. Figure 8 also emphasizes that the CaCO_3 particles are much larger than the cells formed from the individual latex particles. It would be very unlikely that these large particles could act as an obstacle to intercellular polymer diffusion. The retardation that is observed at very high pigment levels is likely related to relatively strong

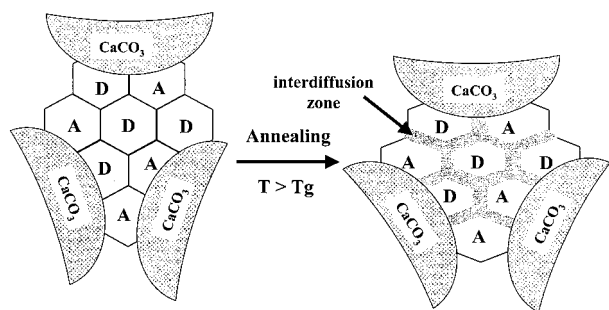


Figure 8. Schematic representation of the annealing process for a latex film containing precipitated calcium carbonate. The latex particles spread locally along the pigment surface.

interactions between the polymer and the pigment surface, which increases the rigidity of the adjacent polymer.

Joanicot et al.⁶ examined the binder–pigment morphology of such systems. They spread a carboxyl-functionalized styrene–butyl acrylate latex dispersion on a calcium carbonate crystal plate and observed it by atomic force microscopy (AFM). They used the same surface coverage as in typical matte paint, which has a pigment volume concentration of 70%. They showed that the binder spreads along the crystal surface, but that the latex polymer particles never form continuous films unless they are annealed at very high temperature. They concluded that, in the actual coating, the CaCO_3 pigments can be fixed by isolated latex particles, i.e., stuck together at many discrete points.

In our case, the latex particles are not acid-functionalized, but we can provide a few further insights into this model. We know from our measurements on newly formed films that $\Phi_{\text{ET}}(0)$ does not change as the fraction of pigment in the system increases. From this result, we have inferred that the interfacial area between donor- and acceptor-labeled cells does not change significantly, even when there is 90 wt % pigment. The pigment, of course, is more dense, so that 90 wt % pigment corresponds to about 25 vol % binder. When these samples are annealed, polymer diffusion leads to an increase in Φ_{ET} , but the last stages of mixing are strongly retarded. As one can see in Table 3, 112 h of annealing for 90 wt % CaCO_3 , even at 60 °C, leads to $\Phi_{\text{ET}} = 0.36$ and $f_m(t) = 0.53$. We interpret this result as indicating that, upon annealing, the droplet of latex film shown in Figure 8 spreads locally along the pigment surface. In this way, we imagine that a significant fraction of the polymer molecules adsorb to the polymer surface in such a way that they do not participate in the polymer interdiffusion process.

It is always possible that pigment surfaces interact differently with the chromophores than with the polymer backbone. This effect would be very difficult to measure, but selective adsorption would be analogous to processes involved in adsorption chromatography. If this were the case, one could rationalize the result seen at long annealing times in the film containing 90 wt % CaCO_3 . If polymer diffusion were accompanied by flow along the pigment surface, then chromophore adsorption might lower the fraction of donor and acceptor groups able to participate in energy transfer.

Another aspect of our measurements that one should keep in mind is that our films are opaque. Our experiments measure fluorescence in the reflectance mode from the samples. The excitation light might penetrate

into the sample to a depth not much larger than the wavelength of light. Thus, we might be observing selectively processes that occur in the first 1 μm of these 100- μm -thick films.

Summary

We employed the fluorescence energy-transfer technique to measure the rate of polymer interdiffusion in latex films formed in the presence of large amounts of inorganic pigment. We found that the presence of different amounts of CaCO_3 and silica pigment had almost no effect on the initial efficiency of energy transfer. This surprising result indicates that, despite the rather substantial contact between pigment and polymer in the films, the presence of pigment has little effect on the total interfacial area between donor- and acceptor-labeled particles in the newly formed film. This result also indicates that the presence of the pigment does not promote coalescence of the latex particles. Small amounts of CaCO_3 have little effect on the polymer diffusion rate in the binder phase, but at very high solids content (80–90 wt %), the diffusion rate is slowed. In contrast, 25-nm-diameter silica particles have a much more pronounced effect on slowing the rate of polymer diffusion. Because of sample brittleness, we could study films containing only up to 50 wt % silica. In these films, the binder is present as the continuous phase. At 90 wt % CaCO_3 , the volume fraction of binder is about 0.25. Here, the binder serves primarily to glue the pigment particles together. Because of the air voids in the matrix, these films are essentially opaque.

Acknowledgment. The authors thank the Surface Science Consortium at the Pulp and Paper Center, University of Toronto, for their support of this research. M.K. thanks Oji Paper Co., Ltd., for his stay in Toronto. The authors thank Okutama Kogyo Co., Ltd., for kindly supplying a calcium carbonate slurry and Clariant Corporation for kindly supplying a colloidal silica dispersion.

References and Notes

- (1) Macnair, A. K. *Synthetic Coating Adhesives*; TAPPI Press: Atlanta, GA, 1998.
- (2) LePoutre, P. *Prog. Org. Coat.* **1989**, *17*, 89.
- (3) (a) Wang, Y.; Kats, A.; Juhue, D.; Winnik, M. A. *Langmuir* **1992**, *8*, 1435. (b) Winnik, M. A. The Formation and Properties of Latex Films. In *Emulsion Polymerization and Emulsion Polymers*; Lovell, P. A., El-Aasser, M. S., Eds.; Wiley: New York, 1997. (c) Keddie, J. L. *Mater. Sci. Eng.* **1997**, *21*, 101.
- (4) (a) Granier, V.; Sartre, A. *Langmuir* **1995**, *11*, 2179. (b) Butt, H. J.; Gerharz, B. *Langmuir* **1995**, *11*, 4735. (c) Unertl, W. N. *Langmuir* **1998**, *14*, 2201. (d) Sheehan, J. G.; Whalen-Shaw, M. *Tappi J.* **1990**, *73*, 171.
- (5) (a) Sheehan, J. G.; Takamura, K.; Davis, H. T.; Scriven, L. E. *Tappi J.* **1993**, *76*, 93. (b) Ming, Y.; Davis, H. T.; Scriven, L. E.; Takamura, K.; Vodnick, J. L. *TAPPI 1995 Coating Conference Proceedings*; TAPPI Press: Atlanta, GA, 1995; p 391.
- (6) Joanicot, M.; Granier, V.; Wong, K. *Prog. Org. Coat.* **1997**, *32*, 109.
- (7) (a) Förster, Th. *Ann. Phys. (Leipzig)* **1948**, *2*, 55. (b) Lakowicz, J. R. *Principles of Fluorescence Spectroscopy*; Plenum Press: New York, 1983.
- (8) (a) Zhao, C.-L.; Wang, Y.; Hruska, Z.; Winnik, M. A. *Macromolecules* **1990**, *23*, 4082. (b) Farinha, J. P. S.; Martinho, J. M. G.; Kawaguchi, S.; Yekta, A.; Winnik, M. A. *Macromolecules* **1995**, *28*, 6084. (c) Kim, H.; Winnik, M. A. *Macromolecules* **1995**, *28*, 2033. (d) Winnik, M. A.; Pineng, P.; Krüger, C.; Zhang, J.; Yaneff, P. V. *J. Coat. Technol.* **1999**, *71*, 47.
- (9) Feng, J.; Odobina, E.; Winnik, M. A. *Macromolecules* **1998**, *31*, 5290.

- (10) Feng, J.; Winnik, M. A. *Macromolecules* **1997**, *30*, 4324.
- (11) Feng, J. Ph.D. Thesis, University of Toronto, Toronto, Canada, 1997.
- (12) Liu, R.; Kobayashi, M.; Winnik, M. A. Unpublished results, 1999.
- (13) Rharbi, Y.; Cabane, B.; Vacher, A.; Joanicot, M.; Boue, F. *Europhys. Lett.* **1999**, *46*, 472.
- (14) O'Connor, D. V.; Phillips, D. *Time-correlated Single Photon Counting*; Academic Press: New York, 1984.
- (15) Martinho, J. M. G.; Egan, L. S.; Winnik, M. A. *Anal. Chem.* **1987**, *59*, 861.
- (16) (a) Wang, Y.; Zhao, C.; Winnik, M. A. *J. Chem. Phys.* **1991**, *95*, 2143. (b) Wang, Y.; Winnik, M. A.; Haley, F. *J. Coat. Technol.* **1992**, *64*, 51. (c) Kim, H.; Wang, Y.; Winnik, M. A. *Polymer* **1994**, *35*, 1779. (d) Kim, H.; Winnik, M. A. *Macromolecules* **1994**, *27*, 1007.
- (17) (a) Joanicot, M.; Wong, K.; Maquet, J.; Chevalier, Y.; Pichot, C.; Graillat, C.; Lindner, P.; Rios, L.; Cabane, B. *Prog. Colloid Polym. Sci.* **1990**, *81*, 175. (b) Chevalier, Y.; Pichot, C.; Graillat, C.; Joanicot, M.; Wong, K.; Lindner, P.; Cabane, B. *Colloid Polym. Sci.* **1992**, *270*, 806.
- (18) Pham, H. H.; Farinha, J. P. S.; Winnik, M. A. *Macromolecules* **2000**, *33*, 5850.
- (19) Farinha, J. P. S.; Martinho, J. M. G.; Yekta, A.; Winnik, M. A. *Macromolecules* **1995**, *28*, 6084.
- (20) Wang, Y.; Winnik, M. A. *J. Phys. Chem.* **1993**, *97*, 2507.
- (21) Wang, Y.; Winnik, M. A. *Macromolecules* **1993**, *26*, 3147.
- (22) (a) Klein, J.; Fletcher, D. *Nature* **1983**, *304*, 526. (b) Bartels, C. R.; Crist, B., Jr.; Fetters, L. J.; Graessley, W. W. *Macromolecules* **1986**, *19*, 785. (c) Shull, K. R.; Kramer, E. J.; Fetters, L. J. *Nature* **1990**, *345*, 790. (d) Shull, K. R.; Dai, K. H.; Kramer, E. J.; Fetters, L. J.; Antonietti, M.; Sillescu, H. *Macromolecules* **1991**, *24*, 505. (e) Gell, C. B.; Graessley, W. W.; Efstratiadis, V.; Pitsikalis, M. *J. Polym. Sci.: Polym. Phys.* **1997**, *35*, 1943.
- (23) Farinha, J. P. S.; Vorobyova, O.; Winnik, M. A. *Macromolecules* **2000**, *33*, 5863.
- (24) Odrobina, E.; Feng, J.; Pham, H. H.; Winnik, M. A. *Macromolecules*, manuscript submitted.
- (25) (a) O'Brien, J.; Cashell, E.; Wardell, G.; McBrierty, V. J. *Macromolecules* **1976**, *9*, 653. (b) Douglass, D.; McBrierty, V. J. *Polym. Eng. Sci.* **1979**, *19*, 1054. (c) Ito, M.; Nakamura, T.; Tanaka, K. *J. Appl. Polym. Sci.* **1985**, *30*, 3493. (d) Dutta, N.; Choudhury, N.; Haidar, B.; Vidal, A.; Donnet, J.; Delmotte, L.; Chezeau, J. *Polymer* **1994**, *35*, 4293. (e) Pliskin, I.; Tokita, N. *J. Appl. Polym. Sci.* **1972**, *16*, 473.
- (26) (a) Tsagaropoulos, G.; Eisenberg, A. *Macromolecules* **1995**, *28*, 396. (b) Tsagaropoulos, G.; Eisenberg, A. *Macromolecules* **1995**, *28*, 6067.
- (27) Mackie, J. S.; Meares, P. *Proc. R. Soc. London A* **1955**, *232*, 498.

MA000604N